Chapter 12
Geometrical and Topological Dimensions of the Diamond

G.V. Zhizhin, Z. Khalaj, and M.V. Diudea

Abstract The question of possible existence of molecules in spaces of higher dimensions, as a consequence of special distribution of matter, is addressed. The geometrical features of the adamantane molecule are examined in detail. It is shown that the adamantane molecule has the dimension 4. The connection ways of the adamantane molecules are investigated on the basis of their geometric properties. Topological properties of the diamond, a 3-periodic net of adamantane, and of a hyperdiamond, called diamond D_5, are given in terms of Omega and Cluj polynomials.

12.1 Introduction

Carbon is one of the most important natural elements in the periodic table, in a variety of millions of compounds and forms. There are four valance electrons in the carbon atom, two in the 2s orbital and two in the 2p orbitals. When combine, these orbitals lead to three types of hybrid orbitals: sp, sp^2, and sp^3 ones. The electronic and atomic arrangements enable carbon to exist in different allotropes such as diamond, diamond-like carbon, graphite, fullerenes, nanotubes, nanowalls, etc. Some of these allotropes are shown in Fig. 12.1 (Khalaj et al. 2012; Khalaj and Ghoranneviss 2012).

Diamond D_6, the classical diamond, is an all-hexagonal ring network, of sp^3 hybridized carbon atoms with adamantane and diamantane the repeating units, as

G.V. Zhizhin
Member of "Skolkovo" OOO "Adamant", Saint-Petersburg, Russia

Z. Khalaj
Department of Physics, Shahr-e-Qods Branch, Islamic Azad University, Tehran, Iran

M.V. Diudea (✉)
Department of Chemistry, Faculty of Chemistry and Chemical Engineering, Babes-Bolyai University, Arany Janos Street 11, Cluj-Napoca RO-400028, Romania
e-mail: diudea@chem.ubbcluj.ro

A.R. Ashrafi, M.V. Diudea (eds.), *Distance, Symmetry, and Topology in Carbon Nanomaterials*, Carbon Materials: Chemistry and Physics 9,
DOI 10.1007/978-3-319-31584-3_12

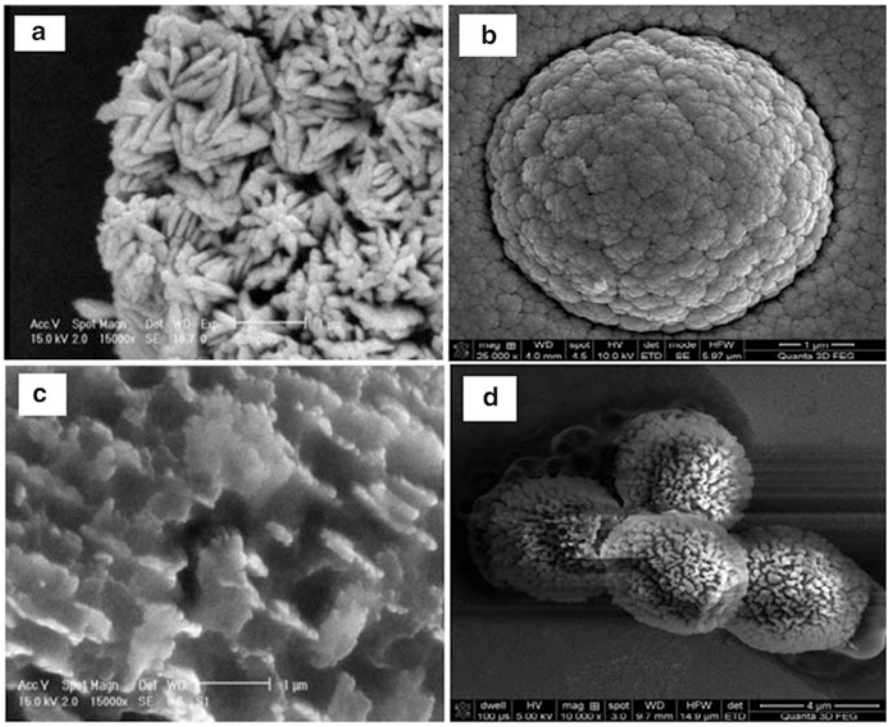

Fig. 12.1 Some of the carbon allotropes synthesized using different CVD systems: (**a**) self-assembled cone-like carbon, (**b**) cauliflower diamond-like carbon, (**c**) carbon nanowalls, (**d**) carbon microspheres

shown in Fig. 12.2; it is crystallized in a face-centered cubic *fcc* network (space group $Fd3m$).

Diamond has kept its highest importance among the carbon allotropes, in spite of many "nano" varieties appeared in the last years (Decarli and Jamieson 1961; Osawa 2007, 2008; Williams et al. 2007; Dubrovinskaia et al. 2006). Its physical characteristics: high thermal conductivity, large band gap, excellent hardness, high electrical resistivity, and low friction coefficient (Takano et al. 2005; Yamazaki et al. 2008), led to outstanding applications in electronics, optics, mechanics, etc. (Sharda et al. 2001). Composites including diamonds may overpass the resistance of steel or metal alloys. Synthetic diamonds can be produced by a variety of methods, including high pressure-high temperature HPHT, static or detonating procedures, chemical vapor deposition CVD (Lorentz 1995), ultrasound cavitation (Khachatryan et al. 2008), or mechanosynthesis (Merkle and Freitas 2003; Sourina and Korolev 2005; Tarasov et al. 2011).

Hyperdiamonds are covalently bonded carbon phases, more or less related to the diamond network, having a significant amount of sp^3 carbon atoms. Their physical properties are close to that of the classical diamond, sometimes with exceeding

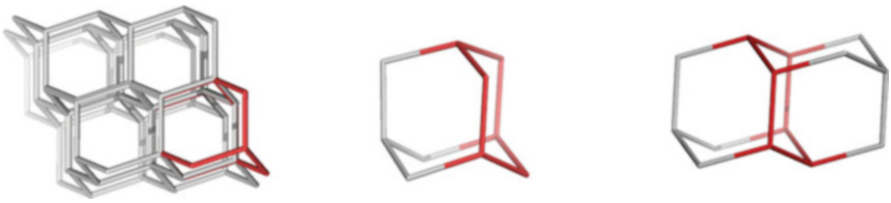

Fig. 12.2 Diamond D_6 (*left*), adamantane D_6_10 (*left*), diamantane D_6_14 (*middle*), and diamond D_6_52 (a 222 Net – *right*)

hardness and/or endurance. In this respect, the hyperdiamond D_5 will be presented in Sect. 12.5.

The chapter is structured as follows. After the introductory part, the main hypotheses of the space and matter will be introduced in Sect. 12.2. Next, the dimension of adamantane molecule is investigated in detail in Sect. 12.3, while its connecting ways evaluated in Sect. 12.4. Section 12.5 introduces the hyperdiamond D_5, while Sects. 12.6 and 12.7deal with the topology of diamonds D_6 and D_5 in terms of Omega and Cluj polynomials, respectively. Conclusions and references will close the chapter.

12.2 Space and Matter

The space in mathematics is a logically conceivable form (or structure) that serves as a medium in which there are other forms or structures (Mathematical encyclopedia 1984). In this definition, it is essential that the space is a logically conceivable form. Visual image of any object on the retina of the human eye is two dimensional. By this reason, any object is perceived initially as a two-dimensional one. Similarly, we only touch the surface of objects, that is, again the palpable image of objects has the dimensionality two. The representation as three-dimensional forms only comes out as a result of the comparison of the mismatched images in the right and left eye, this difference being stronger observed in motion; the comparison is a result of thinking, of the rational. Although many people traditionally consider the world around us as three dimensional, it is only an abstract submission. It should be kept in mind that the geometrical axioms are neither synthetic a priori judgments nor experimental facts.

There are only contingent provisions: when choosing among all possible provisions, we are guided by experimental facts, but the choice is free and limited only by the need to avoid any controversy (Poincare' 1902).

Historically, there were two main concepts of space. In their frames, there are a set of modifications and corresponding geometries. The first idea, associated with the names of Aristotle and Leibniz, is that the real space is a property of the material provision of the objects. As a result, it is linked inextricably with the matter. The development of this idea led to the known position of the philosophy that *there is no space without matter* just as there is no matter without space. The space is a form of

existence of the matter. The second of these ideas, associated with the names of Democritus and Newton, is that the space is the repository of all material objects, which do not have any influence on the space (Einstein 1930). It was the defining idea for many centuries and the philosophical basis of Euclidean geometry (Euclid 2012). In accordance with it, the geometric space is continuous, endless, three dimensional, homogeneous (all points in space are identical to each other), and isotropic (all lines passing through one point are identical to each other). N. I. Lobachevsky (and independently, Bolyai) suggested a non-Euclidean geometry (Lobachevsky 1835). In accordance with this, there can be more than one parallel line through a point outside the line in the plane. This new geometry connected with physics, space, and matter. B. Riemann (1868) extended the geometry of Lobachevsky. He developed the idea of nonhomogeneous spaces, while their connection with the matter follows to the formation of space structure. Here Riemann idea merges with the concept of Leibniz, according to which the space is a property of the position of material objects. Riemannian nonhomogeneous spaces were realized in Einstein's physical theory of general relativity, which provided scientific proof of natural relationship of space and matter. It is believed that the issues of space heterogeneity and the emergence of high-dimensional spaces are important only for large-scale objects such as our universe and larger. The modern theory on the universal nature of the world (superstring theory) easily uses the concept of the nine-dimensional space (Atwood et al. 2008; Burgess and Quevedo 2008; Green 2011; Zwiebach 2011). However, in the near-to-us space, as the biosphere, we can find higher-dimension space objects with a specific distribution of atoms.

Modern researches show that the three-dimensional model of our world often leads to contradictions. For example, the three-dimensional space model could not certainly describe the experimental electron diffraction patterns of quasi crystals (intermetallic compounds) (Janssen et al. 2007). Only four-dimensional space model explains it (Shevchenko et al. 2013a, b; Zhizhin 2014a, b). Experimental studies of phase transitions of the second kind can be explained only by assuming the four-dimensional space (Landau 1937; Kadanoff 1966; Wilson 1971a, b; Fischer and Pfeuty 1972). Such phase transitions in solids occur not only in labs but also in the nature, for example, in the formation of rocks.

Clathrate compounds (i.e., inclusion compounds) are widely occurring in the nature. They are formed by inclusion of some molecules in the cavities of crystal lattices of molecules of another type (lattice clathrates), or in the cavities of another type of molecules (molecular clathrates). An important example of the lattice clathrate is the methane hydrate. In it, the methane molecules are enclosed in thevoids of the crystal lattice of ice. Reserves of methane on the ocean floor in this form are probably much higher than the gas reserves in a free state. Studies on clathrates with silicon and germanium atoms indicate a possible four-dimensional of these compounds (Adams et al. 1994; Nagy and Diudea 2013; Ashrafi et al. 2013). Many natural minerals exist in the nature in the form of fused different geometric shapes passing through each other. It also could be the formation of higher-dimensional geometric shapes. As it is known, the diamond unit cell could be identified through various polyhedra, such as tetrahedron, octahedron, and others (Shafranovsky 1964).

12.3 Dimension of Adamantane Molecule

In this section, the question of the dimensionality of a molecule is considered in detail in the case of adamantane. As a chemical compound, adamantane was discovered in 1933 (Landa and Machacek 1933). Adamantane molecule consists of 10 carbon atoms, a repeating unit of carbon atoms in the crystal lattice of diamond, and 16 hydrogen atoms. The hydrogen atoms are connected to carbon atoms on the unsaturated valences of the carbon atoms. Derivatives of adamantane (e.g., amantadine, memantine, rimantadine, tromantadine) have found practical applications in medicine (as antiviral, antispasmodics, anti-Parkinson drugs, etc.). Among the inorganic and organometallic compounds, there is a number of structural analogs of adamantane, such as phosphorus oxide, urotropine, and others. In 2005, a silicon analogue of adamantane has been synthesized (Fischer et al. 2005). The adamantane structure is a common one in the literature (Bauschlicher et al. 2007; Dahl et al. 2003 – see Fig. 12.2, middle).

Spicing about the adamantane molecule, we often keep in mind exactly ten carbon atoms of the molecule adamantane, although, strictly speaking, it is only a part of the adamantane molecule. However, this figure is a little informative and does not reflect the main features of the spatial arrangement of atoms.

Theorem (Zhizhin 2014c) The adamantane molecule is a convex polytope in the 4D space.

Proof We shall build an adamantane cell in the 3D Euclidean space by imposing the condition: six atoms from ten carbon atoms of adamantane be located in the center of planar faces of the cube.

Each of the remaining four carbon atoms inside the cube is equidistant to the three centers of the nearest flat faces of the cube (Fig. 12.3). In Fig. 12.3 one can see thin solid lines delineating the regular tetrahedron inscribed in the cube. Its edges are the diagonals of the cube faces. The solid thick lines correspond to the covalent bonds between carbon atoms. We suppose that the carbon atoms, in the vertices of the cube, are arranged as in the diamond structure. Other substance possible arrangement of carbon atoms in the vertices of a cube will not influence the analysis on the geometry of adamantane. The dotted line passing through the points α_2, α_6, α_3, α_4, α_8, and α_9 delineate a regular octahedron with its vertices located in the center of the cube faces and sharing some vertices with the adamantane. Barcode dotted lines delineate the regular tetrahedron whose vertices coincide with the carbon atoms of adamantane, located inside the cube α_1, α_5, α_7, and α_{10}. By construction, the formed segments connecting the vertices of adamantane split into ten families of parallel lines, each family of three parallel segments: (1) $\alpha_1\alpha_2$, $\alpha_7\,\alpha_6, \alpha_{10}\alpha_9$; (2) $\alpha_3\alpha_1$, $\alpha_8\ \alpha_{10}, \alpha_5\alpha_6$; (3) $\alpha_3\alpha_2$, $\alpha_7\ \alpha_5, \alpha_8\alpha_9$; (4) $\alpha_1\alpha_4$, $\alpha_7\ \alpha_8, \alpha_5\alpha_9$; (5) $\alpha_4\alpha_2$, $\alpha_8\ \alpha_6, \alpha_{10}\alpha_5$; (6) $\alpha_9\alpha_2$, $\alpha_3\ \alpha_8, \alpha_{10}\alpha_1$; (7) $\alpha_4\alpha_3$, $\alpha_7\ \alpha_{10}, \alpha_6\alpha_9$; (8) $\alpha_5\alpha_2$, $\alpha_7\ \alpha_3, \alpha_{10}\alpha_4$; (9) $\alpha_1\alpha_5$, $\alpha_3\ \alpha_6, \alpha_4\alpha_9$; and (10) $\alpha_6\alpha_2$, $\alpha_7\ \alpha_1, \alpha_4\alpha_8$. Consequently, the total number of segments, each of which is an edge of a polyhedron, is equal to 30. The length of the segments is determined by the length of the cube

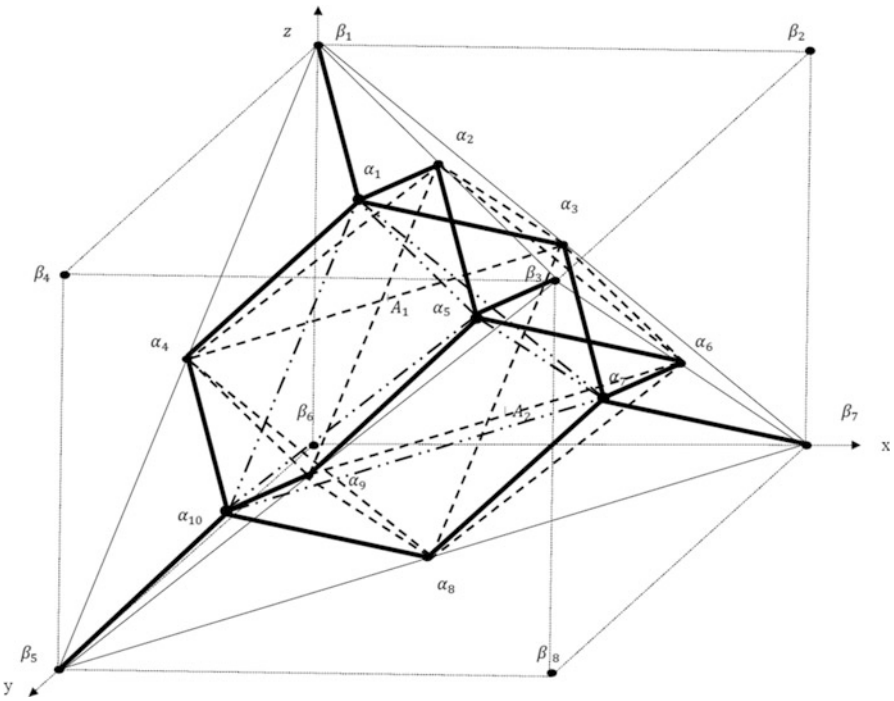

Fig. 12.3 Structure of adamantane

edges. Put the length of cube edge equal to 1 (to go to the specific dimensions of the bond length must enter a scale factor). Then a regular tetrahedron with the bases on the faces of the octahedron and the vertices in the vertices of the cube (e.g., a tetrahedron $\beta_1\alpha_2\alpha_3\alpha_4$) will have the length $a = 1/\sqrt{2}$ and the radius of the circle around the tetrahedron $b = \sqrt{3}$ / 4 (the points α_2; α_6, α_3; and α_4 ,α_8 , α_9 are in the centers of the cube faces). Therefore, segments 2, 5, 6, 7, 9, and 10 have the length a, while the segments 1, 3, 4, and 8 have the length b. Thus, the two-dimensional geometric elements involved in adamantane are the lengths of sides a and b.

One can define (Fig. 12.3) a set of two-dimensional faces belonging to the adamantane, forming a regular triangle with sides a, an isosceles triangle with the base a and two sides b, squares with sides a, and a rectangle with sides a and b. Among the regular triangles, there are 4 triangles located at the outer edge of adamantane ($\alpha_2\alpha_3\alpha_6$, $\alpha_2\alpha_4\alpha_9$, $\alpha_4\alpha_3\alpha_8$, $\alpha_9\alpha_8\alpha_6$) and 8 triangles located in the inner part of adamantane ($\alpha_1\alpha_5\alpha_{10}$, $\alpha_1\alpha_7\alpha_{10}$, $\alpha_1\alpha_7\alpha_5$, $\alpha_2\alpha_9\alpha_6$, $\alpha_2\alpha_3\alpha_4$,$\alpha_8\alpha_3\alpha_6$, $\alpha_4\alpha_9\alpha_8$, $\alpha_5\alpha_{10}\alpha_7$). Among the irregular triangles, there are 12 triangles located at the outer edge of adamantane ($\alpha_2\alpha_3\alpha_1$, $\alpha_2\alpha_1\alpha_4$, $\alpha_1\alpha_3\alpha_4$, $\alpha_2\alpha_5\alpha_9$, $\alpha_2\alpha_5\alpha_6$, $\alpha_3\alpha_7\alpha_8$, $\alpha_3\alpha_7\alpha_6$, $\alpha_4\alpha_{10}\alpha_9$, $\alpha_4\alpha_{10}\alpha_8$, $\alpha_5\alpha_9\alpha_6$, $\alpha_7\alpha_8\alpha_6$, $\alpha_8\alpha_9\alpha_{10}$) and 6 triangles located in the inner part of adamantane ($\alpha_1\alpha_4\alpha_{10}$, $\alpha_2\alpha_5\alpha_1$, $\alpha_5\alpha_6\alpha_7$, $\alpha_1\alpha_7\alpha_3$, $\alpha_{10}\alpha_5\alpha_9$, $\alpha_7\alpha_8\alpha_{10}$). Thus, there is a total of 30 triangles in adamantane. In the inner part of adamantane, there are three squares of side a, as the three sections of the octahedron

($\alpha_2\alpha_6\alpha_8\alpha_4, \alpha_2\alpha_3\alpha_8\alpha_9, \alpha_3\alpha_6\alpha_9\alpha_4$), and 12 parallelograms (Fig. 12.3) with sides a and b ($\alpha_1\alpha_3\alpha_8\alpha_{10}$, $\alpha_1\alpha_2\alpha_9\alpha_{10}$, $\alpha_1\alpha_5\alpha_9\alpha_4$, $\alpha_1\alpha_7\alpha_8\alpha_4, \alpha_1\alpha_3\alpha_5\alpha_6, \alpha_1\alpha_7\alpha_6\alpha_2, \alpha_2\alpha_4\alpha_5\alpha_{10}$, $\alpha_7\alpha_3\alpha_2\alpha_5, \alpha_7\alpha_3\alpha_4\alpha_{10}, \alpha_5\alpha_6\alpha_8\alpha_{10}, \alpha_5\alpha_7\alpha_8\alpha_9$, $\alpha_6\alpha_7\alpha_9\alpha_{10}$).

These parallelograms are rectangles, as one can prove that wrong plane triangles, based on the specified side of the squares, are perpendicular to the plane of these squares. Indeed, one may cut up the adamantane by a plane passing, for example (see Fig. 12.3), through the top $\alpha_2$and the edges $\alpha_1\alpha_2$, and α_2 α_5 (due to the symmetry of the octahedron and tetrahedron built on its edges, these edges lie in the same plane). This plane cuts up irregular triangles $\alpha_1\alpha_3\alpha_4$, $\alpha_5\alpha_9\alpha_6$ and regular triangles $\alpha_2\alpha_3\alpha_4$, $\alpha_6\alpha_8\alpha_9$on their height, passing through the middle of the edges $\alpha_3\alpha_4$ and $\alpha_6\alpha_9$ (respectively, the points A_1, A_2 in Fig. 12.3) and vertex α_8. Intersection plane is presented in Fig. 12.4. We prove that the segments $\alpha_1A_1$and α_3A_2 are perpendicular on the line A_1A_2. This will prove the wrong triangle perpendicular to the plane of the square plane $\alpha_6\alpha_3\alpha_9\alpha_4$. Let us consider the triangle $\alpha_2\alpha_3$ A_2; in it $A_1A_2 = a$ and $\alpha_2A_2 = b = \frac{\sqrt{6}}{4}a$, $A_2\alpha_3 = \frac{a}{2\sqrt{2}}$.

Therefore, $\cos\angle\alpha_2A_2\alpha_3 = \sqrt{\frac{2}{3}}$ and $\sin\angle\alpha_2A_2\alpha_3 = \frac{1}{\sqrt{3}}$. From the triangle $A_1A_2\alpha_2$, one can see that $\cos\angle\alpha_2A_2A_1 = \frac{1}{\sqrt{3}}$, $\sin\angle\alpha_2A_2A_1 = \sqrt{\frac{2}{3}}$. Consequently, $\cos(\angle\alpha_2A_2\alpha_3 + \angle\alpha_2A_2A_1) = 0$. Then, $\alpha_3A_2 \perp A_1A_2$. This also implies that $\alpha_1\alpha_3 \perp \alpha_3\alpha_6$ and $\alpha_5\alpha_6 \perp \alpha_3\alpha_6$; in other words the parallelogram $\alpha_3\alpha_6\alpha_1\alpha_5$ is a rectangle. One can prove that the remaining parallelograms are also rectangles. Thus, the number of squares and rectangles is 15, and the total number of geometric elements of dimension 2 consisting of adamantane is 45.

These 2D geometric elements form in adamantane 25 of 3D polyhedron (Fig. 12.3):

Five tetrahedron ($\alpha_4\alpha_3\alpha_1\alpha_2$, $\alpha_{10}\alpha_7\alpha_1\alpha_5$, $\alpha_4\alpha_{10}\alpha_9\alpha_8, \alpha_3\alpha_6\alpha_7\alpha_8$, $\alpha_2\alpha_6\alpha_9\alpha_5$)

Six prisms ($\alpha_3\alpha_2\alpha_1\alpha_8$ $\alpha_9\alpha_{10}$, $\alpha_6\alpha_2\alpha_1\alpha_7$ $\alpha_9\alpha_{10}$, $\alpha_3\alpha_2\alpha_5\alpha_8$ $\alpha_9\alpha_7$, $\alpha_3\alpha_5\alpha_1\alpha_8$ $\alpha_6\alpha_{10}$, $\alpha_5\alpha_2\alpha_6\alpha_8$ $\alpha_4\alpha_{10}$, $\alpha_5\alpha_4\alpha_1\alpha_8$ $\alpha_9\alpha_7$)

Fourteen pyramids ($\alpha_4\alpha_2\alpha_1\alpha_9\alpha_{11}$, $\alpha_5\alpha_2\alpha_1\alpha_9\alpha_{10}$, $\alpha_4\alpha_3\alpha_1\alpha_8\alpha_{10}$, $\alpha_7\alpha_3\alpha_1\alpha_8\alpha_{10}$, $\alpha_4\alpha_2\alpha_3\alpha_9\alpha_8$, $\alpha_3\alpha_2\alpha_6\alpha_9\alpha_8$, $\alpha_3\alpha_2\alpha_1\alpha_5\alpha_6$, $\alpha_5\alpha_3\alpha_1\alpha_6\alpha_7$, $\alpha_4\alpha_3\alpha_6\alpha_9\alpha_8$, $\alpha_4\alpha_2\alpha_3\alpha_9\alpha_6$, $\alpha_4\alpha_3\alpha_1\alpha_7\alpha_{10}$, $\alpha_4\alpha_3\alpha_7\alpha_8\alpha_{10}$, $\alpha_4\alpha_5\alpha_1\alpha_9\alpha_{10}$,$\alpha_4\alpha_2\alpha_1\alpha_9\alpha_5$)

Calculation of 3D octahedron, as consisting from two pyramids, was not considered, because the square section of the octahedron is involved in the formation of other 3D shapes. We now calculate Euler's formula for the polytope P of dimension n (Poincare 1895; Grunbaum 1967) by substituting the number of figures/shapes of various dimensions included in adamantane: $\sum_{j=0}^{n-1}(-1)^j f_j(P) = 1 + (-1)^{n-1}$, $f_j(P)$ being the number of figures of dimension j in the polytope P.

As shown above, in this case we have $f_0(P) = 10$, $f_1(P) = 30$, $f_2(P) = 45$, $f_3(P) = 25$. All the elements of dimension 3 are convex (including 3D boundary of the points set), and no elements of dimension greater than 3 exists within the adamantane. Substituting the values obtained for the number of figures of different dimension in Euler's formula, for $n = 4$, we have 10–30 + 45–25 = 0. This proves the theorem.

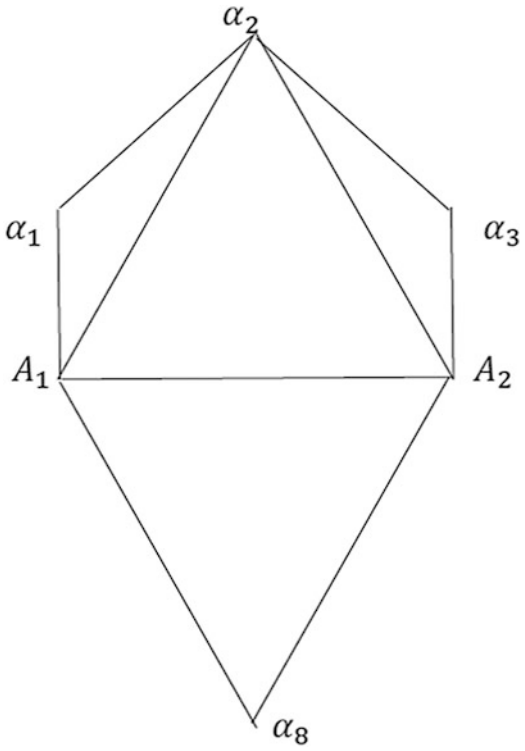

Fig. 12.4 Section of adamantane

Thus, adamantane is a convex polytope of dimension 4. From each vertex this polytope outlets 6 rays as in the 16-cell convex regular 4D polytope (Grunbaum 1967; Zhizhin 2014a). All two-dimensional faces of adamantane are simultaneously faces of two 3D shapes, indicating the isolation of adamantane as a polytope. The outer boundary of adamantane consisting of two-dimensional faces of the polytope is the projection of the polytope on the 3D space, just as the outer boundary of any closed polytope on 2D plane is a closed circuit composed of one-dimensional segments.

12.4 Connection Ways of Adamantane Molecules

In view of the established geometric properties of adamantane molecules, they can join to each other by three ways: (1) at the vertices located at the centers of cube faces; (2) at the wrong parallel triangle; and (3) at the broken hexagonal contours formed by the right triangle and its surrounding irregular triangle constituting the dihedral angles with the right triangle.

12.4.1 The First Way of Joining Adamantane Molecules

It leads to the standard model of translational diamond with the *fcc* unit cell. The coordinates of the adamantane vertices are calculated as integers. Indeed, if we shall take the unit cell edge length equal to 4, the coordinates *x, y*, and *z* of vertices in the initial position (denoted by the subscript 0, $\alpha_{i,\,0}(x_{i,\,0},\, y_{i,\,0},\, z_{i,\,0})$) in Fig. 12.3 are $\alpha_{1,0}(1, 1, 3)$, $\alpha_{2,0}(2, 2, 4)$, $\alpha_{3,0}(2, 0, 2)$, $\alpha_{4,0}(0, 2, 2)$, $\alpha_{5,\,0}(3, 3, 3)$, $\alpha_{6,\,0}(4, 2, 2)$, $\alpha_{7,\,0}(3, 1, 1)$, $\alpha_{8,\,0}(2, 2, 0)$, $\alpha_{9,\,0}(2, 4, 2)$, $\alpha_{10,\,0}(1, 3, 1)$. Then, to translate the cube on $k(k_x, k_y, k_z)$ steps toward *x, y*, and *z* coordinates, formula for computing these new vertex positions is

$$\alpha_{i,\,k}\left(x_{i,\,k},\, y_{i,\,k},\, z_{i,\,k}\right) = \alpha_{i,k}\left(x_{i,\,0} + 4k_x,\, y_{i,0} + 4k_y,\, z_{i,\,0} + 4k_z\right);\;\; i = 1,\, 2,\, \ldots, 10;$$

k_x, k_y, k_z being integers (positive and negative). As it was shown above, for determining the coordinates of adamantane in integers, it is not necessary to use the theory of numbers, as was done in the work of (Balaban 2013).

On the set of cubic cells of adamantane molecules, one can establish the existence of a scaling process, diamond scaling, i.e., formation of large-scale geometric shapes of the same figures as in the smaller scale. For the first time, the process of scaling was detected at the phase transitions of the second kind (Kadanoff 1966). Also it was detected on the grid of hyperrombohedron vertices in quasicrystals (Zhizhin 2014a, b).

Figure 12.5 shows the scaling with an octahedron based on eight cubes, each containing 8 times smaller octahedron. This explains the existence of diamond crystals of macroscopic dimensions with the same form as the microscopic unit cell of diamond. The increase in scale occurs in a discrete manner. Scale crystal diamond increases atn^3 $(n = 1,\, 2,\, \ldots.)$ strokes.

12.5 The Second Way of Joining Adamantane Molecules

As shown in Sect. 12.3, the planes of irregular triangles are perpendicular to the plane of the square section of octahedron. Therefore, adamantane molecules can attach to each other, within an irregular triangle, in two mutually perpendicular directions. Thus, they form a layer of infinite adamantane polyhedra contacting by the free vertices of the octahedron. In such a case, two adamantane molecules adopt a dihedral angle, equal to the dihedral angle between irregular triangles in the adamantane polyhedron. Therefore, in the space of three adamantane polyhedra, contacting the wrong triangles, another adamantane polyhedron can be tightly nested. These form an infinite layer filled by adamantane polyhedra and regular tetrahedra, with a fundamental domain consisting of an adamantane polyhedron and a regular tetrahedron.

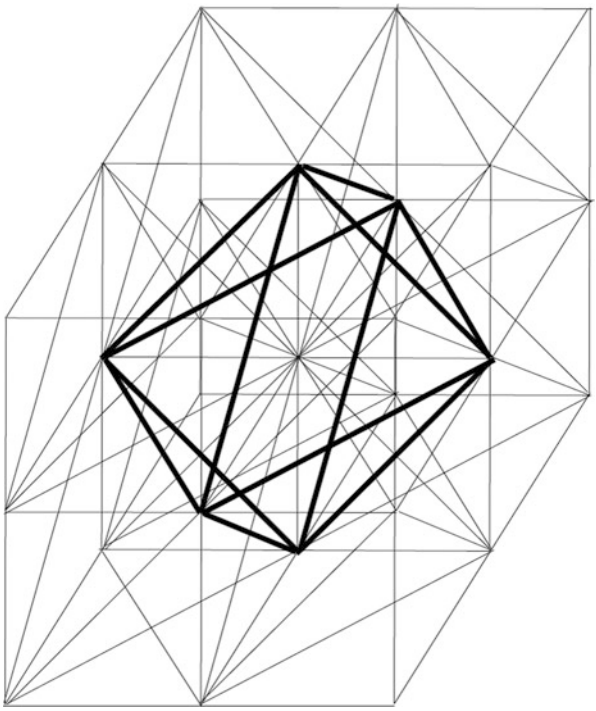

Fig. 12.5 Scaling in diamond

These layers, contacted to each other, completely fill the space. At top view such a layer is shown in Fig. 12.6 (thick lines designate valence bonds). One can see that the condition of four valence carbon atoms in all the vertices was fulfilled, as in the four valence bond carbon atoms, directed from layer to layer (vertically). The distribution of carbon atoms, as shown in Fig. 12.6, describes the oblique coordinate system. The density of this carbon atom arrangement must be higher than the density of the *fcc* diamond fundamental domain.

12.5.1 The Third Way of Connecting Adamantane Molecules

The adamantane polyhedra can communicate with each other besides the tops and irregular triangles also by the broken hexagonal spatial contours whose edges correspond to the valence bonds. The boundary of each adamantane consists of four of these circuits. Combining the two adamantane on such a contour, we obtain the diamantane. A next connection leads to triamantane and so on. Based on this mechanism, a general formula for diamondoids is available (Bauschlicher et al. 2007; Dahl et al. 2003): C_nH_{n+6}, $n = 4i + 6$, $i = 1, 2, \ldots$.

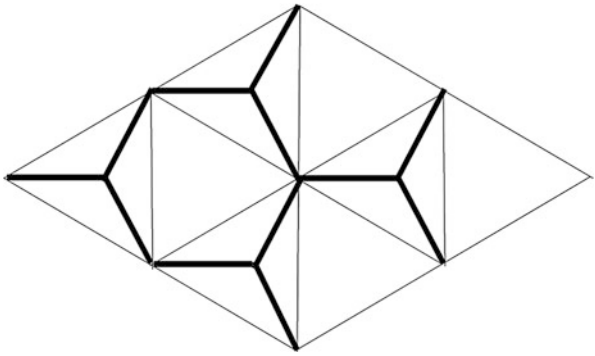

Fig. 12.6 Adamantane compound in an oblique lattice

These diamondoids are shells of the hexagonal loops. Significantly, these coatings may be connected to the carbon structures derived by the second method. This may provide even more complex and diverse compounds.

12.6 Structures of Diamond D_5

A diamondoid crystal structure, with pentagon/hexagon rings, of which 90 % pentagons, was called (Diudea and Nagy 2013) diamond D_5; it is also known as the clathrate II, or *mtn*, and is a 3-periodic, 3-nodal net, of point symbol {5^5.6}12 {5^6}5 and 2[5^{12}]; [$5^{12}.6^4$], a tiling that belongs to the space group $Fd\text{-}3\,m$. The clathrate II structure exists in the synthetic zeolite ZSM-39 (Meyer and Olson 1992), in silica (Böhme et al. 2007; Adams et al. 1994) and in germanium allotrope Ge(*cF*136) (Guloy et al. 2006; Schwarz et al. 2008) as real substances.

Substructures of D_5 are related to the classical D_6 diamond (Diudea et al. 2012; Böhme et al. 2007). An adamantane-like structure D_5_ada can form two diamantane-like D_5_dia forms: anti and syn (Fig. 12.1). Next, D_5_dia_anti substructure will form a 3-periodic *fcc*-crystal network (Benedek and Colombo 1996) (Fig. 12.1, bottom, right), while D_5_dia_syn will self-arrange into a starlike quasicrystal (Diudea 2013) (Fig. 12.1, bottom, left).

Topology of D_5_*anti* in a triclinical domain (*k*,*k*,*k*) (see Fig. 12.7) is presented in Table 12.1: formulas to calculate the number of atoms and number of rings R and the limits (at infinity) for the ratio R_5/all rings are given function of *k* (i.e., the number of repeating units in the domain) (Diudea et al. 2012).

The hyperdiamond D_5 mainly consists of sp^3 carbon atoms building ada-like repeating units (C_{20} cages including C_{28} as hollows). The ratio $C - sp^3/C$-total trends to 1 in a large-enough network. The content of pentagons R[5] per total rings trends to 90 % (see Table 12.1) and, by this reason, this allotrope was called the diamond D_5. For comparison, in this table, topology of diamond D_6 net is included.

Considering the hexagons as "window faces" to the C_{28} hollows, one can evaluate the genus of D_5 net according to the following.

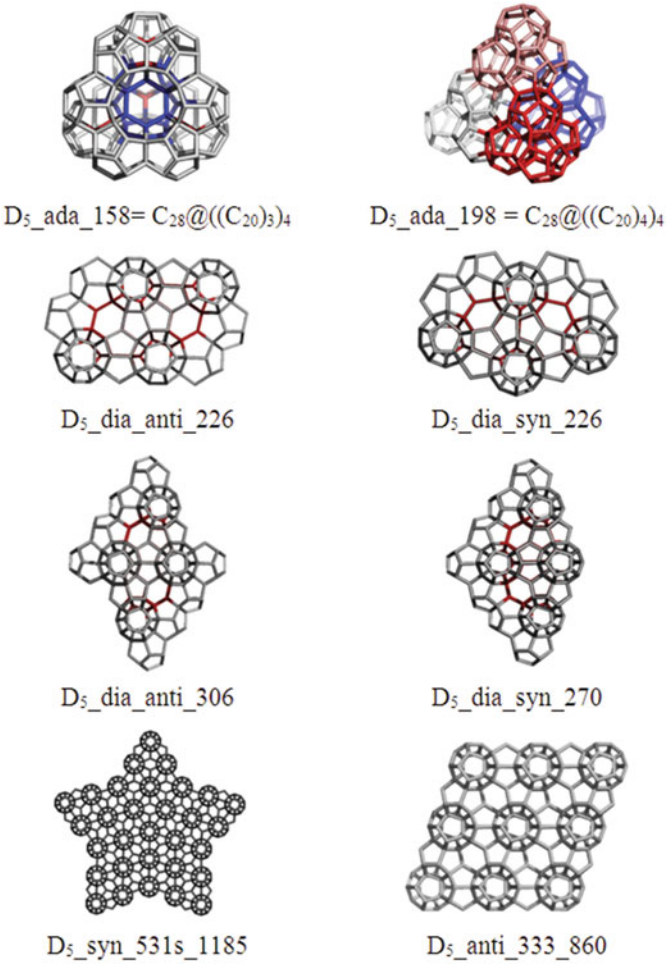

Fig. 12.7 Structures of diamond D_5

Theorem (Diudea and Szefler 2012): In spongy structures built up from u tube junction units, of genus g_u, the genus is calculated as $g = u(g_u - 1) + 1$, irrespective of the unit tessellation.

Data are given in Table 12.2.

Design of the crystal networks herein discussed was performed by using our software programs CVNET (Stefu and Diudea 2005) and NANO-STUDIO (Nagy and Diudea 2009). Topological data were provided by NANO-STUDIO.

Table 12.1 Topology of diamonds D5_anti, and D6, as a function of the number of repeating units k ($k = 1, 2,...$) on the edge of a (k, k, k) triclinical domain

Formulas
$v(\mathrm{D_5\_anti}) = -22 - 12k + 34k^3$
$sp^3\mathrm{atoms} = -10 - 36k^2 + 34k^3$
$\mathrm{Ring}[5] = -18 - 6k - 18k^2 + 36k^3$
$\mathrm{Ring}[6] = -1 + 6k - 9k^2 + 4k^3$
$R[5] + R[6] = -19 - 27k^2 + 40k^3$
$\lim_{k\to\infty} \frac{R[5]}{R[5]+R[6]} = 9/10$
$v(D_6) = 6k + 6k^2 + 2k^3$
$sp^3\mathrm{atoms} = -2 + 6k + 2k^3$
$\mathrm{Ring}[6] = 3k^2 + 4k^3$
$\lim_{k\to\infty} \left[\frac{\mathrm{Atoms}(sp^3)}{v(G)} = \frac{-2+6k+2k^3}{6k+6k^2+2k^3}\right] = 1$

Table 12.2 Genus calculation in diamond D_5 substructures

D_5	v	e	$g = 1 + u(g_u - 1)$	g_u	u
$(C_{20})_{12}C_{28}$_Ada_158	158	274	3	1.5	4
$(C_{20})_{18}(C_{28})_2$_Dia_syn_226	226	398	5	2;1.5	3 + 2
$(C_{20})_{18}(C_{28})_2$_Dia_anti_226	226	398	5	1.5	8

12.7 Omega Polynomial of Diamonds D_5 and D_6

Let $G(V,E)$ be a connected bipartite graph, with the vertex set $V(G)$ and edge set $E(G)$. Two edges $e = (x,y)$ and $f = (u,v)$ of G are called *codistant* (briefly: $e\ co\ f$) if $d(x, v) = d(x, u) + 1 = d(y, v) + 1 = d(y, u)$.

For some edges of a connected graph G, the following relations are satisfied (John et al. 2007):

$$e\ co\ e$$

$$e\ co\ f \ \Leftrightarrow\ f\ co\ e$$

$$e\ co\ f\ \&\ f\ co\ h\ \Rightarrow\ e\ co\ h$$

though the last relation is not always valid.

Let $C(e) := \{f \in E(G);\ f\ co\ e\}$ denote the set of edges in G, codistant to the edge $e \in E(G)$. If relation co is an equivalence relation, then G is called a *co-graph*. Consequently, $C(e)$ is called an *orthogonal cut qoc* of G, and $E(G)$ is the union of disjoint orthogonal cuts $C_1 \cup C_2 \cup \ldots \cup C_k$ and $Ci \cap Cj = \emptyset$ for $i \neq j,\ i,j = 1, 2, .., k$.

A *quasi-orthogonal cut qoc* with respect to a given edge is the smallest subset of edges closed undertaking opposite edges on faces. Since the transitivity of the co relation is not necessarily obeyed, *qoc* represents a less constrained condition: any

oc strip is a *qoc* strip but the reverse is not always true. More about Omega polynomial, the reader can find in Chap. 2 of this book.

Let $m(G,c)$ denote the number of *qoc* strips of length c (*i.e.*, the number of cutoff edges); for the sake of simplicity, $m(G,c)$ can be written as m. The Omega polynomial is defined on the ground of *qoc* strips (Diudea 2006):

$$\Omega(G,x) = \sum\nolimits_c m(G,c) \cdot x^c$$

Its first derivative (in $x = 1$) equals the number of edges in the graph:

$$\Omega^{'}(G,1) \quad = \sum\nolimits_c m \cdot c = e = |E(G)|$$

On Omega polynomial, the Cluj-Ilmenau index (John et al. 2007), $CI = CI(G)$, was defined (Diudea 2006):

$$CI(G) = \left\{ \left[\Omega^{'}(G,1)\right]^2 - \left[\Omega^{'}(G,1) + \Omega^{''}(G,1)\right] \right\}$$

Topology of diamond D_5, in a cubic (k,k,k) domain, is presented in Table 12.2 (Diudea et al. 2011): formulas to calculate the number of atoms, number of rings, and the limits (to infinity) for the ratio of sp^3C atoms over total number of atoms and also the ratio $R[5]$ over the total number of rings are given. Tables 12.3 to 12.5 give formulas for calculating Omega polynomial in diamonds D_5 and D_6 and some numerical examples.

12.8 Cluj Polynomial in Diamond D_6

A counting polynomial can be written as

$$P(G,x) = \sum\nolimits_k m(G,k) \cdot x^k$$

where the exponents of indeterminate x show the extent of partition $p(G)$, $\cup p(G) = P(G)$, of a graph property $P(G)$, while the coefficients $m(G,k)$are related to the occurrence of partitions of extent k. Quantum chemistry first used the polynomial description of molecular graphs, namely, the *characteristic polynomial* (Diudea et al. 2002; Aihara 1976; Gutman et al. 1977); its roots represent the energies of the Hűckel*pi*-molecular graphs. Counting polynomials have been introduced in the Mathematical Chemistry literature by Hosoya (1988, 1990; Hosoya and Yamaguchi 1975).

The Cluj polynomials (Diudea 2009; Diudea et al. 2007, 2010a, b, c; Dorosti et al. 2009; Saheli and Diudea 2013) are defined on the basis of Cluj matrices; they count the vertex proximity of a vertex i with respect to any vertex j in G, joined to

Table 12.3 Omega polynomial in diamonds D_5 and D_6 as a function of the number of repeating units k along the edge of a cubic (k,k,k) domain

	Omega(D_5); R[6]
1	$\Omega(D_5, x) = \left(32 - 54k + 36k^2 + 44k^3\right) \cdot x + \left(-3 + 18k - 27k^2 + 12k^3\right) \cdot x^2$
2	$\Omega^{'}(1) = e(G) = -38 - 18k - 18k^2 + 68k^3$
3	$CI(G) = 1488 + 1350k + 1764k^2 - 4612k^3 - 2124k^4 - 2448k^5 + 4624k^6$
	Omega(D_6); R[6]
4	$\Omega(D_6\_k_{odd}, x) = \left(\sum_{i-1}^{k} 2x^{\frac{(i+1)(i+2)}{2}}\right) + \left(\sum_{i-1}^{(k-1)/2} 2x^{\frac{(k+1)(k+2)}{2} + \frac{k \times k-1}{4} - i(i-1)}\right) + 3kx^{(k+1)^2}$
5	$\Omega(D_6\_k_{even}, x) = \left(\sum_{i-1}^{k} 2x^{\frac{(i+1)(i+2)}{2}}\right) + \left(\sum_{i-1}^{k/2} 2x^{\frac{(k+1)(k+2)}{2} + \frac{k \times k}{4} - (i-1)(i-1)}\right) - x^{\frac{(k+1)(k+2)}{2} + \frac{k \times k}{4}} + 3kx^{(k+1)^2}$
6	$\Omega^{'}(1) = e(G) = -1 + 6k + 9k^2 + 4k^3$
7	$CI(G) = 2 - 187k/10 - k^2/4 + 305k^3/4 + 457k^4/4 + 1369k^5/20 + 16k^6$

Table 12.4 Examples, omega polynomial in diamond D_5

K	Omega(D_5); R[6]	Atoms	sp^3Atoms (%)	Bonds	CI	R[5]	R[6]
2	$356\,x^1 + 21\,x^2$	226	118 (52.21)	398	157,964	186	7
3	$1318\,x^1 + 132\,x^2$	860	584 (67.91)	1582	2,500,878	774	44
4	$3144\,x^1 + 405\,x^2$	2106	1590 (75.50)	3954	15,629,352	1974	135
5	$6098\,x^1 + 912\,x^2$	4168	3340 (80.13)	7922	62,748,338	4002	304

Table 12.5 Examples, omega polynomial in diamond D_6

k	Omega(D_6); R[6]	Atoms	sp^3Atoms (%)	Bonds	CI(G)	R [6]
2	$2x^3 + 2x^6 + 1x^7 + 6x^9$	52	26 (50.00)	79	5616	44
3	$2x^3 + 2x^6 + 2x^{10} + 2x^{12} + 9x^{16}$	126	70 (55.56)	206	39,554	135
4	$2x^3 + 2x^6 + 2x^{10} + 2x^{15} + 2x^{18} + 1x^{19} + 12x^{25}$	248	150 (60.48)	423	169,680	304
5	$2x^3 + 2x^6 + 2x^{10} + 2x^{15} + 2x^{21} + 2x^{25} + 2x^{27} + 15x^{36}$	430	278 (64.65)	754	544,746	575

i by an edge (the Cluj-edge polynomials $CJDI_e(x)$) or by a path (the Cluj-path polynomials $CJDI_p(x)$). The coefficients $m(k)$can be calculated from the entries of the corresponding UCJDI matrices by the TOPOCLUJ software program (Ursu and Diudea 2005). The summation runs over all $k = |\{p\}|$in G.

In bipartite graphs, the coefficients of CJ polynomial can be calculated by an orthogonal edge-cut procedure (Diudea et al. 2010a, b; Gutman and Klavžar 1995; Klavžar 2008).

To perform an orthogonal cut, take a straight line segment, orthogonal to the edge e, and intersect e and all its parallel edges in the graph. The set of these intersections is called an *orthogonal cut* $c_k(e)$, $k = 1,2,..,k_{max}$. An example is given in Fig. 12.8. To any orthogonal cut c_k, two numbers can be associated: (i) *number of edges* e_k intersected (i.e., cutting cardinality $|c_k|$) and (ii) v_k or the number of points lying to the left hand with respect to c_k (in round brackets, in Fig. 12.8).

Let us define the *partial cube* as a graph embeddable in the hypercube *n*-cube Q_n, which is a regular graph whose vertices are binary strings of length n, two strings being adjacent if they differ in exactly one position (Harary 1969). The distance function in the *n*-cube is the Hamming distance. A hypercube can be expressed as the Cartesian product: $Q_n = \square_{i=1}^{n} K_2$ where K_2 is the complete graph on two vertices.

For any edge $e = (u,v)$ of G, let n_{uv} denote the set of vertices lying closer to u than to v: $n_{uv} = \{w \in V(G) | d(w,u) < d(w,v)\}$. Then we can write $n_{uv} = \{w \in V(G) | d(w,v) = d(w,u) + 1\}$. The sets (and subgraphs) induced by these vertices, namely, n_{uv} and n_{vu}, are called *semicubes* of G; they are disjoint *opposite semicubes* (Diudea and Klavžar 2010; Diudea et al. 2008).

A graph G is bipartite if and only if, for any edge of G, the opposite semicubes define a partition of G: $n_{uv} + n_{vu} = v = |V(G)|$. These semicubes represent the

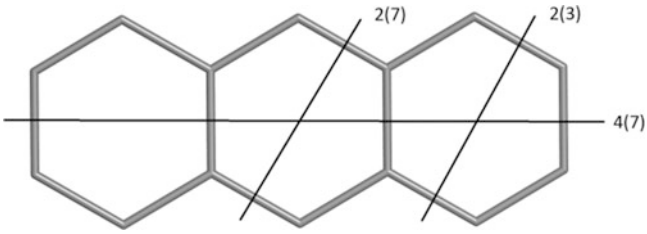

Fig. 12.8 Cutting procedure in Cluj polynomials
$\mathrm{CJS(x)} = 4 \times 2\left(\mathrm{x}^3 + \mathrm{x}^{(14-3)}\right) + 4\left(\mathrm{x}^7 + \mathrm{x}^{(14-7)}\right) + 2 \times 2\left(\mathrm{x}^7 + \mathrm{x}^{(14-7)}\right) = 8\mathrm{x}^{11} + 16\mathrm{x}^7 + 8\mathrm{x}^3$
$\mathrm{CJS}'(1) = 224 = \mathrm{v} \times \mathrm{e} = \mathrm{Sum}(\mathrm{UCJDI_e})_{\mathrm{i,j}}$
$\mathrm{CJP(x)} = 4 \times 2\left(x^{3(14-3)}\right) + 4\left(x^{7(14-7)}\right) + 2 \times 2\left(x^{7(14-7)}\right) = 8x^{49} + 8x^{33}\mathrm{CJP}'(1) = 656 = 1312/2 = (1/2)\mathrm{Sum}(\mathrm{SCJDI}_e)_{i,j}$

vertex proximities of the endpoints of edge $e = (u,v)$, on which *CJ* polynomials are defined. In partial cubes, the semicubes can be estimated by an orthogonal cutting-edge procedure. The orthogonal cuts form a partition of the graph edges

$$E(G) = c_1 \cup c_2 \cup \ldots \cup c_k, \quad c_i \cap c_j = \varnothing, \ i \neq j$$

Let$v = v(G) = |V(G)|$ and $e = e(G) = |E(G)|$ be the cardinality of the vertex and edge sets, respectively. The Cluj polynomials are calculated by recomposing the local contributions (as provided by the cutting procedure) to the global graph property, differing only by the arithmetic operation used (Diudea 2010a, b):

(i) *Cluj-Sum* polynomial, CJS(x), is counted by summation of local contributions (Diudea 2009; Diudea et al. 2007, 2010a):

$$CJS(x) = \sum\nolimits_e \left(x^{v_k} + x^{v-v_k}\right)$$

(ii) *Cluj-Product* polynomial, CJP(x), is counted by the pair-wise product of the cutting contributions (Diudea 1997a, b). It is identical to the *Szeged* polynomial, $SZ_v(x)$ (Gutman 1994; Ashrafi et al. 2008; Khalifeh et al. 2008; Mansour and Schork 2009):

$$CJP(x) = SZ_v(x) = \sum\nolimits_e x^{v_k(v-v_k)}$$

The first derivatives (in $x = 1$) provide single numbers, often called topological indices, characterizing the encoded topological property (e.g., the vertex proximities in the graph); thus, $\mathrm{CJS}'(1) = \mathrm{Sum}(\mathrm{UCJDI_e})_{\mathrm{i,j}}$ and $\mathrm{CJP}'(1) = (1/2)\mathrm{Sum}(\mathrm{SCJDI}_e)_{\mathrm{i,j}}$, respectively.

In case of CJS(x), the following theorem (Diudea 2009; Diudea et al. 2007) is involved:

Theorem The sum of all edge-counted vertex proximities, p_e, in a bipartite graph, is $p_e = v \times e$, i.e., the product of the number of vertices and edges in G.

Demonstration In a bipartite planar graph, which allows orthogonal edge-cuts, for every edge $e(i,j) \in E(G)$, the vertex proximities $\{p_{e,i}\}$ and $\{p_{e,j}\}$ of its endpoints are clearly separation. Denote the cardinalities of the above sets by $p_{e,i}$ and $p_{e,j}$, then

$$p_{e,i} + p_{e,j} = v$$

and next, by summing the contributions of all the edges in G, one obtains the total of vertex proximities, $p_e = v \times e$.

$$\begin{aligned} p_e &= \sum\nolimits_c m(G,c) \cdot c \cdot \left(p_{e,i} + p_{e,j}\right) = \sum\nolimits_c m(G,c) \cdot c \cdot v = e \times v \\ &= \sum\nolimits_{i,j} \left[\mathrm{UCJDI}_e(G)\right]_{i,j} = \mathrm{CJS}'(G,1) \end{aligned}$$

thus demonstrating the theorem.

Corollary In a bipartite graph, there are no equidistant vertices with respect to the two endpoints of any edge.

This is the main result provided by the Cluj matrix/polynomial (Diudea et al. 2007). It was independently discovered in (Došlić and Vukičević 2007) and proposed as the "bipartite edge-frustration" index, a criterion for checking the bipartivity of a graph.

Formulas for calculating Cluj *CJS* polynomial in diamond D_6 are presented in Table 12.6, while Table 12.7 gives some numerical examples (Saheli and Diudea 2013).

Table 12.6 Cluj *CJS* polynomial in diamond D_6

	Cluj polynomial
1	$CJS(x) = \sum_{i=1}^{k} \left(i^2 + 3i + 2\right) \left[x^{\frac{1}{6}i\left(2i^2+9i+13\right)} + x^{2k\left(k^2+3k+3\right)} - \frac{1}{6}i\left(2i^2+9i+13\right)\right]$ $+ \sum_{i=1}^{\left\lfloor \frac{k}{2} \right\rfloor} [(k+1)\,(k+2) + 2i(k-i)] \left[x^{\frac{1}{6}k\left(2k^2+9k+13\right) + ik(3+i+k) + \frac{i}{3}\left(5-2i^2\right)}\right]$ $+ \sum_{i=1}^{\left\lfloor \frac{k}{2} \right\rfloor - 1} [(k+1)(k+2) + 2i(k-i)] \left[x^{\frac{1}{6}k\left(10k^2+27k+23\right) - ik(3+i+k) - \frac{i}{3}\left(5-2i^2\right)}\right]$ $+ \left[\frac{1-(-1)^k}{4}\right] \left(3k^2+6k+3\right) x^{\left(k^3+\frac{15}{4}k^2+\frac{9}{2}k+\frac{3}{4}\right)} + 6(k+1)^2 \sum_{i=1}^{k} x^{2k\left(k^2+3k+3\right)} - 2i(k+1)^2 + 1$
2	$CJS'(1) = 8k^6 + 42k^5 + 90k^4 + 88k^3 + 30k^2 - 6k$

Table 12.7 Examples of Cluj *CJS* polynomial in diamond D_6 Net

k	Polynomial *CJS*	*CJS*′
1	$6x^{10}+24x^{7}+6x^{4}$	252
2	$6x^{48}+12x^{39}+54x^{35}+14x^{26}+54x^{17}+2x^{13}+6x^{4}$	4108
3	$6x^{122}+12x^{113}+20x^{97}+96x^{95}+24x^{75}+96x^{63}+24x^{51}+96x^{31}+20x^{29}+12x^{13}+6x^{4}$	25,956
4	$6x^{244}+12x^{235}+20x^{219}+150x^{199}+30x^{194}+36x^{161}+150x^{149}+38x^{124}+150x^{99}+36x^{87}+30x^{54}+150x^{49}+20x^{29}+12x^{13}+6x^{4}$	104,904

12.9 Conclusions

In this chapter, the possible existence of local spaces of higher dimension (more than 3), of the indissoluble connection of space and matter, of the space as a form of the existence of matter, and of the heterogeneity of this space, was demonstrated. In a previous paper (Zhizhin 2014a, b), it was shown that the experimental electron diffraction patterns of intermetallic compounds (quasi crystals) can be uniquely described by assuming higher dimensions of space for such materials. It was proved here that the dimension of the adamantane molecule (and its derivatives), due to the special distribution of matter (atoms), is equal to 4. From the proven geometric properties of the adamantane, three major ways for the connection of adamantane molecules were proposed. It was shown that the higher-dimension regions can combine with each other to form nanoscale layers. Nevertheless, they are separated in the 3D space. The same mathematical treatment can be applied to diamond D_5, which is basically a type II clathrate.

Design of diamond D_6 and hyperdiamond D_5 crystal networks was performed by using original software programs CVNET and NANO-STUDIO, developed at TOPO GROUP CLUJ. The topology of the networks was described in terms of Omega and Cluj CJS polynomials, respectively, as functions of the net parameter k representing the number of repeating units in a (k,k,k) cuboid.

References

Adams GB, O'Keeffe M, Demkov AA, Sankey OF, Huang Y-M (1994) Wide – band – gap Si in open fourfold – coordinated clathrate structures. Phys Rev B 49:8048–8053

Aihara J (1976) A new definition of Dewar – type resonance energies. J Am Chem Soc 98:2750–2758

Ashrafi A, Ghorbani M, Jalali M (2008) The vertex PI and Szeged indices of an infinite family of fullerenes. J Theor Comput Chem 7:221–231

Ashrafi AR, Koorepazan – Moftakhar F, Diudea MV, Stefu M (2013) Chap. 18: Mathematics of D_5 network. In: Diudea MV, Csaba CL (eds) Diamonds and related nanostructures. Springer, Dordrecht, pp 321–333

Atwood W, Maykeylson P, Ritz S (2008) The window in the extreme universe. In the world of science. Sci Am 3:16–21

Balaban AT (2013) Chap 1: Diamond hydrocarbons and related structures. In: Diudea MV, Csaba CL (eds) Diamonds and related nanostructures. Springer, Dordrecht, pp 1–28

Bauschlicher CW, Liu Y, Ricca A, Mattioda AL, Allamandola LJ (2007) Electronic and vibrational spectroscopy of diamondoids and the interstellar infrared bands between 3.35 and 3.55 μm. Astrophys J 671:458–469

Benedek G, Colombo L (1996) Hollow diamonds from fullerenes. Mater Sci Forum 232:247–274

Böhme B, Guloy A, Tang Z, Schnelle W, Burkhardt U, Baitinger M, Yu G (2007) Oxidation of M_4Si_4 (M = Na, K) to clathrates by HCl or H_2O. J Am Chem Soc 129:5348–5349

Burgess K, Quevedo F (2008) Large space travel on the "roller coaster". In the world of science. Sci Am 3:22–31

Dahl JE, Liu SG, Carlson RMK (2003) Isolation and structures of higher diamondoids, nanometer – sized diamond molecules. Science 229:96–99

Decarli PS, Jamieson JC (1961) Formation of diamond by explosive shock. Science 133:1821–1822

Diudea MV (1997) Cluj matrix invariants. J Chem Inf Comput Sci 37:300–305

Diudea MV (2006) Omega polynomial. Carpath J Math 22:43–47

Diudea MV (2009) Cluj polynomials. J Math Chem 45:295–308

Diudea MV (2010a) Counting polynomials in partial cubes. In: Gutman I, Furtula B (eds) Novel molecular structure descriptors – theory and applications I. University of Kragujevac, Kragujevac, pp 191–215

Diudea MV (2010b) Counting polynomials and related indices by edge cutting procedures. In: Gutman I, Furtula B (eds) Novel molecular structure descriptors – theory and applications II. University of Kragujevac, Kragujevac, pp 57–78

Diudea MV (2013) Hyper – graphenes. Int J Chem Model 5:211–220

Diudea MV, Klavžar S (2010) Omega polynomial revisited. Acta Chim Sloven 57:565–570

Diudea MV, Nagy CL (eds) (2013) Diamond and related nanostructures, vol 6, Carbon materials: chemistry and physics. Springer, Dordrecht

Diudea MV, Szefler B (2012) Nanotube junctions and the genus of multi – tori. Phys Chem Chem Phys 14(22):8111–8115

Diudea MV, Gutman I, Jäntschi L (2002) Molecular topology. Nova, New York

Diudea MV, Vizitiu AE, Janežič D (2007) Cluj and related polynomials applied in correlating studies. J Chem Inf Model 47:864–874

Diudea MV, Cigher S, John PE (2008) Omega and related counting polynomials. MATCH Commun Math Comput Chem 60:237–250

Diudea MV, Ilić A, Ghorbani M, Ashrafi AR (2010a) Cluj and PI_v polynomials. Croat Chem Acta 83:283–289

Diudea MV, Dorosti N, Iranmanesh A (2010b) Cluj Cj polynomial and indices in a dendritic molecular graph. Studia Univ "Babes–Bolyai"Chemia 55(4):247–253

Diudea MV, Nagy CL, Žigert P, Klavžar S (2010c) Cluj and related polynomials in tori. Studia Univ "Babes–Bolyai"Chemia 55(4):113–123

Diudea MV, Ilić A, Medeleanu M (2011) Hyperdiamonds: a topological view. Iranian J Math Chem 2:7–29

Diudea MV, Nagy CL, Bende A (2012) On diamond D_5. Struct Chem 23:981–986

Dorosti N, Iranmanesh A, Diudea MV (2009) Computing the Cluj index of dendrimer nanostars. MATCH Commun Math Comput Chem 62(2):389–395

Došlić T, Vukičević D (2007) Computing the bipartite edge frustration of fullerene graphs. Discret Appl Math 155:1294–1301

Dubrovinskaia N, Dub S, Dubrovinsky L (2006) Superior wear resistance of aggregated diamond nanorods. Nano Lett 6:824–826

Einstein A (1930) The problem of space, fields and ether in physics. Dia Koralle 5:486–487

Euclid (2012) Beginnings. URSS, Moscow

Fischer J, Baumgartner J, Marschner C (2005) Synthesis and structure of sila – adamantane. Science 310:825–830

Fisher ME, Pfeuty P (1972) Critical behavior of the anisotropic n–vector model. Phys Rev B 6:1889–1891

Greene B (2011) Theelegant universe. Superstrings, hidden dimensions and the quest for the ultimate theory. Librokom, Moscow
Grunbaum B (1967) Convexpolytopes. Springer, London
Guloy A, Ramlau R, Tang Z, Schnelle W, Baitinger M, Yu G (2006) A quest – free germanium clathrate. Nature 443:320–323
Gutman I (1994) A formula for the Wiener number of trees and its extension to graphs containing cycles. Graph Theory Notes of NY 27:9–15
Gutman I, Klavžar S (1995) An algorithm for the calculation of the Szeged index of benzenoid hydrocarbons. J Chem Inf Comput Sci 35:1011–1014
Gutman I, Milun M, Trinajstić N (1977) Graph theory and molecular orbitals. 19. Nonparametric resonance energies of arbitrary conjugated systems. J Am Chem Soc 99:1692–1704
Harary F (1969) Graph theory. Addison – Wesley, Reading
Hosoya H (1988) On some counting polynomials in chemistry. Discret Appl Math 19:239–257
Hosoya H (1990) Clar's aromatic sextet and sextet polynomial. Top Curr Chem 153:255–272
Hosoya H, Yamaguchi T (1975) Sextet polynomial. A new enumeration and proof technique for the resonance theory applied to the aromatic hydrocarbons. Tetrahedron Lett 16(52): 4659–4662
Janssen T, Chapuis G, De Boissieu M (2007) Aperiodic crystals. From modulated phases to quasicrystals. Oxford University Press, Oxford
John PE, Vizitiu AE, Cigher S, Diudea MV (2007) CI index in tubular nanostructures. MATCH Commun Math Comput Chem 57:479–484
Kadanoff LP (1966) Scaling laws for Isingmodels near τ_c^* Physics 2:263–272
Khachatryan AK, Aloyan SG, May PW, Sargsyan R, Khachatryan VA, Baghdasaryan VS (2008) Graphite-to-diamond transformation induced by ultrasound cavitation. Diam Relat Mater 17:931–936
Khalaj Z, Ghoranneviss M (2012) Investigation of metallic nanoparticles produced by laser ablation method and their catalytic activity on CVD diamond growth. Studia Univ "Babes−Bolyai"Chemia 57(2):21–28
Khalaj Z, Ghoranneviss M, Vaghri E, Saghaleini A, Diudea MV (2012) Deposition of DLC film on stainless steel substrates coated by Nickel using PECVD method. Acta Chim Slov 59:338–343
Khalifeh M, Yousefi – Azari H, Ashrafi A (2008) A matrix method for computing Szeged and vertex PI indices of join and composition of graphs. Linear Algebra Appl 429:2702–2709
Klavžar S (2008) A bird's eye view of the cut method and a survey of its applications in chemical graph theory. MATCH Commun Math Comput Chem 60:255–274
Landa S, Machacek V (1933) Sur l'adamantane, nouvel hydrocarbure extait du naphte. Collection Czech Commun 5:1–5
Landau LD (1937) On the theory of phase transitions I. J Exp Theor Phys 7:19–38
Lobachevsky NI (1835) Imaginary geometry. Sci Notes Kazan Univ 1:3–88
Lorenz HP (1995) Investigation of TiN as an interlayer for diamond deposition on steel. Diam Relat Mater 4:1088–1092
Mansour T, Schork M (2009) The vertex PI index and Szeged index of bridge graphs. Discret Appl Math 157:1600–1606
Mathematical encyclopedia 4 (1984) Sov encyclopedia, Moscow
Meier WM, Olson DH (1992) Atlas of zeolite structure types, 3rd edn. Butterworth – Heineman, London
Merkle RC, Freitas RA Jr (2003) Theoretical analysis of a carbon-carbon dimer placement tool for diamond mechanosynthesis. J Nanosci Nanotechnol 3(4):319–324
Nagy CL, Diudea MV (2009) NANO–studio software program. Babes–Bolyai University, Cluj
Nagy CL, Diudea MV (2013) Chap 5: Diamond D_5. In: Diudea MV, Csaba CL (eds) Diamonds and related nanostructures. Springer, Dordrecht, pp 91–106
Osawa E (2007) Recent progress and perspectives in single – digit nano diamond. Diam Relat Mater 16:2018–2022
Osawa E (2008) Monodisperse single nano diamond particulates. Pure Appl Chem 80:1365–1379

Poincaré A (1895) Analysis situs. J de Ecole Polyt 1:1–121
Poincaré A (1902) La science et Chypothe'se. Flammarion, Paris
Riemann B (1868) On the hypotheses underlying geometry. Gëtt. Abhandlungen 13
Saheli M, Diudea MV (2013) Chap. 10: Cluj and other polynomials of D_6 and related networks. In: MV Diudea, CL Nagy (eds) Carbon materials: chemistry and physics, 6: Diamond and related nanostructures, Springer, Dordrecht, Heidelberg, New York, London, pp 191–204
Schwarz U, Wosylus A, Böhme B, Baitinger M, Hanfland M, Yu G (2008) A 3D network of four – bonded germanium: a link between open and dense. Angew Chem Int Ed 47:6790–6793
Shafranovsky II (1964) Diamonds. Nauka, Moscow – Leningrad
Sharda T, Rahaman MM, Nukaya Y, Soga T, Jimbo T, Umeno M (2001) Structural and optical properties of diamond and nano–diamond films grown by microwave plasma chemical vapor deposition. Diam Relat Mater 10:561–467
Shevchenko VYA, Zhizhin GV, Mackay A (2013a) On the structure of quasicrystals in the space of higher dimension. News RAS Chem Ser 2:269–274
Shevchenko VYA, Zhizhin GV, Mackay A (2013b) Chapter 17: On the structure of the quasicrystals in the high dimention space. In: Diamonds and related nanostructures. Springer, Dordrecht, pp 311–320
Sourina O, Korolev N (2005) Design and analysis of a molecular tool for carbon transfer in mechanosynthesis. J Comput Theor Nanosci 2(4):492–498
Stefu M, Diudea MV (2005) CageVersatile_CVNET software program. Babes–Bolyai University, Cluj
Takano Y, Nagao M, Takenouchi T, Umezawa H, Sakaguchi I, Tachiki M, Kawarada H (2005) Superconductivity in polycrystalline diamond thin films. Diam Relat Mater 14:1936–1938
Tarasov D, Izotova E, Alisheva D, Akberova N, Freitas RA Jr (2011) Structural stability of clean, passivated, and partially dehydrogenated cuboid and octahedral nanodiamonds up to 2 nanometers in size. J Comput Theor Nanosci 8:147–167
Ursu O, Diudea MV (2005) TopoCluj software program. Babes–Bolyai University Cluj, Cluj
Williams OA, Douhéret O, Daenen M, Haenen K, Osawa E, Takahashi M (2007) Enhanced diamond nucleation on monodispersed nanocrystalline diamond. Chem Phys Lett 445:255–258
Wilson RG (1971a) Renormalization group and critical phenomena. I. Renormalization group and the Kadanoff scaling picture. Phys Rev B 4:3174–3183
Wilson RG (1971b) Renormalization group and critical phenomena. II. Phase-space cell analysis of critical behavior. Phys Rev B 4:3184–3205
Yamazaki K, Furuichi K, Tsumura I, Takagi Y (2008) The large–sized diamond single–crystal synthesis by hot filament CVD. J Cryst Growth 310:1019–1022
Zhizhin GV (2014a) World 4D. Polytechnic Service, St. Petersburg
Zhizhin GV (2014b) Disproportionate and fluctuating structure in space earthly reality. Biosphere 3:211–221
Zhizhin GV (2014c) On higher dimension in nature. Biosphere 4:1–10
Zwiebach B (2011) Initial course theory string. URSS, Moscow